JOURNAL OF Evolutionary Biology

doi: 10.1111/jeb.13209

The divergence history of the perennial plant *Linaria cavanillesii* confirms a recent loss of self-incompatibility

M. VOILLEMOT*, Q. ROUGEMONT†, C. ROUX*‡ & J. R. PANNELL*

*Department of Ecology and Evolution, Biophore/Sorge, University of Lausanne, Lausanne, Switzerland
†Institut de Biologie Intégrative et des Systèmes (IBIS), University of Laval, Québec City, Québec, Canada
‡Unité Evo-Eco-Paléo (EEP) - UMR 8198, CNRS, Université de Lille Sciences et Technologies, Villeneuve d'Ascq Cedex, France

Keywords:

approximate Bayesian computation simulations;
mating system transition;
population divergence;
purging;
self-compatibility;
selfing syndrome.

Abstract

Many angiosperms prevent inbreeding through a self-incompatibility (SI) system, but the loss of SI has been frequent in their evolutionary history. The loss of SI may often lead to an increase in the selfing rate, with the purging of inbreeding depression and the ultimate evolution of a selfing syndrome, where plants have smaller flowers with reduced pollen and nectar production. In this study, we used approximate Bayesian computation (ABC) to estimate the timing of divergence between populations of the plant *Linaria cavanillesii* that differ in SI status and in which SI is associated with low inbreeding depression but not with a transition to full selfing or a selfing syndrome. Our analysis suggests that the mixed-mating self-compatible (SC) population may have begun to diverge from the SI populations around 2810 generation ago, a period perhaps too short for the evolution of a selfing syndrome. We conjecture that the SC population of *L. cavanillesii* is at an intermediate stage of transition between outcrossing and selfing.

Introduction

Hermaphrodite plants have evolved numerous strategies to prevent self-fertilization and thus to avoid the deleterious effects of inbreeding depression (Barrett, 2002). One of the most effective of these is self-incompatibility (SI), a genetic system leading to the rejection of pollen grains by pistils carrying the same alleles at the self-incompatible locus (S-locus) (Castric & Vekemans, 2004; Franklin-Tong, 2008; Shimizu & Tsuchimatsu, 2015). SI is widespread in flowering plants (60% of angiosperm species are considered SI, Igic & Kohn, 2006), but many species have independently evolved self-compatibility (SC) through the breakdown of SI. Indeed, the loss of SI probably represents one of the most common evolutionary transition to have occurred in the history of angiosperms (Stebbins, 1974; Igic *et al.*, 2008; Goldberg *et al.*, 2010; Wright & Barrett, 2010). Understanding why some populations are resistant to the establishment of SC individuals, whereas SC fixes in others, is central to our quest to understand the diversity of plant mating systems.

Two main reasons have been given to explain the frequent independent transitions from SI to SC. The first invokes a direct fitness advantage gained by SC individuals that pass an extra copy of their genes to the next generation by self-fertilizing their progeny (automatic selection hypothesis; Fisher, 1941). Mutations conferring SC and increased selfing should thus spread in a population in the absence of countervailing forces, such as inbreeding depression (Charlesworth & Charlesworth, 1987) or pollen discounting, whereby self-fertilization compromises a plant's outcrossing potential (Nagylaki, 1976; Holsinger, 1988; Harder & Barrett, 1995; Harder & Wilson, 1998; Porcher & Lande, 2005).

The second reason invokes an advantage of reproductive assurance (Darwin, 1876; Lloyd, 1965; Jain, 1976; reviewed in Busch & Delph, 2012). In SI individuals, the number of available partners depends both on population size and the presence of external vectors to move pollen from one individual to another. In small and isolated populations, SI alleles can be lost by drift (Wright, 1939), so that different individuals are more likely to carry the same alleles and therefore to reject each other's outcross pollen, with consequently lost mating opportunities (Charlesworth & Charlesworth, 1979; Busch &

Correspondence: John R. Pannell, Department of Ecology and Evolution, Biophore/Sorge, University of Lausanne, 1015 Lausanne, Switzerland.
Tel.: +41 21 692 4170; fax: +41 21 692 4165;
e-mail: john.pannell@unil.ch

Schoen, 2008; Young & Pickup, 2010; Stone *et al.*, 2014). Mates may also be limited during episodes of colonization, where single individuals establish at new localities (Baker, 1955; Pannell, 2015; Pannell *et al.*, 2015). Similarly, in environments where pollinators are scarce, obligate outcrossing individuals will be less able to reproduce than their closely related SC counterparts (Baker, 1955; Cheptou & Massol, 2009; Massol & Cheptou, 2011), even if selfing leads to inbreeding depression (e.g. Herlihy & Eckert, 2002; but see Layman *et al.*, 2017). SC may also confer an outcrossing advantage, particularly in small populations, because SC individuals can mate with any individuals in the population, whereas SI individuals will be prevented from mating with individuals with the shared S-alleles.

Major changes are expected to follow a transition from SI to SC and a concomitant increase in the selfing rate. First, deleterious mutations are expected to be purged by selection, thus resulting in decreased inbreeding depression (Lande & Schemske, 1985; Barrett & Charlesworth, 1991). Although purging may be quick, especially if the transition to selfing coincides with strong bottlenecks (e.g. Busch, 2005a; Guo *et al.*, 2009; Ness *et al.*, 2010), many partially selfing species may maintain high levels of inbreeding depression for long periods (Winn *et al.*, 2011). This might be because inbreeding depression in such populations is so strong that no selfed individuals survive to reproductive maturity, thus removing any possibility for selection among selfed progeny that differ in their load of deleterious mutations (Lande *et al.*, 1994). Alternatively, inbreeding depression might require a longer period of time to be purged (Busch, 2005a).

Because plants that are able to self-fertilize autonomously do not need pollinators, the evolution of SC and self-fertilization is often associated with the evolution of a reduced investment in pollinator attraction and reward, such as through smaller flowers, lower pollen/ovule ratios and reduced nectar production (Ornduff, 1969; Goodwillie *et al.*, 2010; Sicard & Lenhard, 2011). This 'selfing syndrome' has been reported in numerous plant species (reviewed in Goodwillie *et al.*, 2010) and appears to be able to evolve rapidly after a transition to SC and self-fertilization (Bodbyl Roels & Kelly, 2011). However, not all SC species show a shift in flower morphology towards the selfing syndrome (e.g. Busch, 2005b; Fenster & Martén-Rodríguez, 2007; Dart *et al.*, 2012). The reasons for this variation are not well understood and understanding the dynamic of its evolution thus remains interesting.

The consequences and timing of a transition to SC have been investigated in a number of cases where related species or populations differ in their SI status. For instance, *Capsella grandiflora* (Foxe *et al.*, 2009; Guo *et al.*, 2009), *Clarkia xantiana* spp. *parviflora* (Runions & Geber, 2000) and *Arabidopsis thaliana* (Tang *et al.*, 2007) are SC species that show a selfing syndrome and have been recently derived from their SI-related species (Runions & Geber, 2000; Foxe *et al.*, 2009). Coalescent-based analyses have revealed that *Leavenworthia alabamica,* a predominantly SI species, experienced a transition to SC in at least two of its populations more recently than 150 000 years ago, with the most recent transition (about 48 000 years ago) associated with negligible changes in floral morphology (Busch *et al.*, 2011). Similarly, Foxe *et al.* (2010) inferred that some populations of *Arabidopsis lyrata* probably evolved higher selfing rates as recently as 10 000 years ago, also without showing any accompanying shift towards a selfing syndrome.

The perennial herb *Linaria cavanillesii* shows variable levels of SI among its populations and underwent a recent breakdown of its gametophytic SI system in part of its range (Voillemot & Pannell, 2016). The one known SC population of *L. cavanillesii* appears to be at an intermediate step of its evolution from SI to self-fertilization. On the one hand, whereas occasional selfing in the SI population is accompanied by high inbreeding depression, inbreeding depression is absent in the SC population (Voillemot & Pannell, 2017). On the other hand, the SC population continues to show substantial outcrossing (selfing rate $s = 0.59$; Voillemot & Pannell, 2016), a situation in which the purging of inbreeding depression might be ineffectual (Winn *et al.*, 2011). Nor does the SC population show any evidence of a selfing syndrome, with plants from both SC and SI populations producing large flowers with a long nectar-containing spurs, and no reduction in pollen production (Voillemot & Pannell, 2016).

We hypothesized that maintenance of an outcrossing syndrome in *L. cavanillesii* despite its loss of SI and inbreeding depression might be attributable to a very recent transition towards SC. Accordingly, we used an approximate Bayesian computation framework (ABC) (Beaumont *et al.*, 2002) to infer the time of divergence between SI and SC populations of *L. cavanillesii* on the basis of molecular variation at 16 microsatellite loci. ABC uses coalescent simulations to generate genetic data expected under a given demographic model. Simulated data are then compared with observed data to test the relevance of the demographic model, bypassing the need to compute full likelihoods – a major limitation for most demographic models (Beaumont *et al.*, 2002; Csilléry *et al.*, 2010). Our results confirm that the SC population of *L. cavanillesii* is very recently derived from neighbouring SI populations and indeed represents one of the most recent transitions from outcrossing to partial selfing yet documented.

Materials and methods

Study species

Linaria cavanillesii is a perennial herb endemic to southeastern Spain. Plants grow on north–northwest-oriented

cliffs at sites ranging from 300 to 1400 m in altitude. Between May and June, individuals grow multiple herbaceous shoots from a subwoody perennial base, with inflorescences developing towards the end of the branches. Yellow flowers have long floral nectar spurs and are pollinated by a variety of bees and bumblebees. Around 30 days after fertilization, mature capsules open and seeds are dispersed passively, probably aided by wind.

Sampled populations

Six populations of *L. cavanillesii* have been the focus of detailed previous analysis (Voillemot & Pannell, 2016): a fully SC population (COV), two SI populations (BER, DEN) and three mixed populations with both SI and leaky SI plants (BUI, RUB, ZAR) (Voillemot & Pannell, 2016). The species has a strong population-genetic structure, with mean pairwise $F_{ST} = 0.56$ (min $F_{ST} = 0.32$, max $F_{ST} = 0.75$), and, for the SC population in particular, high divergence from each of the two closest and northernmost SI populations ($F_{ST} = 0.63$ and 0.56 for COV-DEN and COV-BER, respectively; Voillemot & Pannell, 2016). Population structure combined with preliminary simulations involving all pairs of populations (Fig. S1) suggests that the SC population diverged recently from one of the two closest populations. We thus focused our investigation on these three northern populations (i.e. the SC COV population, and BER and DEN SI populations; Fig. 1).

Genotyping

We collected leaf material from 28 to 41 individuals from each of the three natural populations and extracted DNA with the DNeasy 96 Plant kit (Qiagen, Hombrechtikon, Germany). Sixteen polymorphic microsatellite markers were amplified by PCR (Biometra thermocycler) using the following reagents: 1 × PCR mix: 2 ng μL^{-1} template DNA, 10 × PCR Buffer, 25 mM $MgCl_2$, 5 × Q-solution, 2.5 mM dNTP, 0.2 μM of each primer and 0.5 U μL^{-1} of Taq DNA polymerase (HotStarTaq®; Qiagen). The thermocycling conditions were set to 15 min at 95° followed by 32 cycles of 30 s at the annealing temperature (Voillemot & Pannell, 2016), 30 s at 72 °C and 30 s at 95 °C, followed by

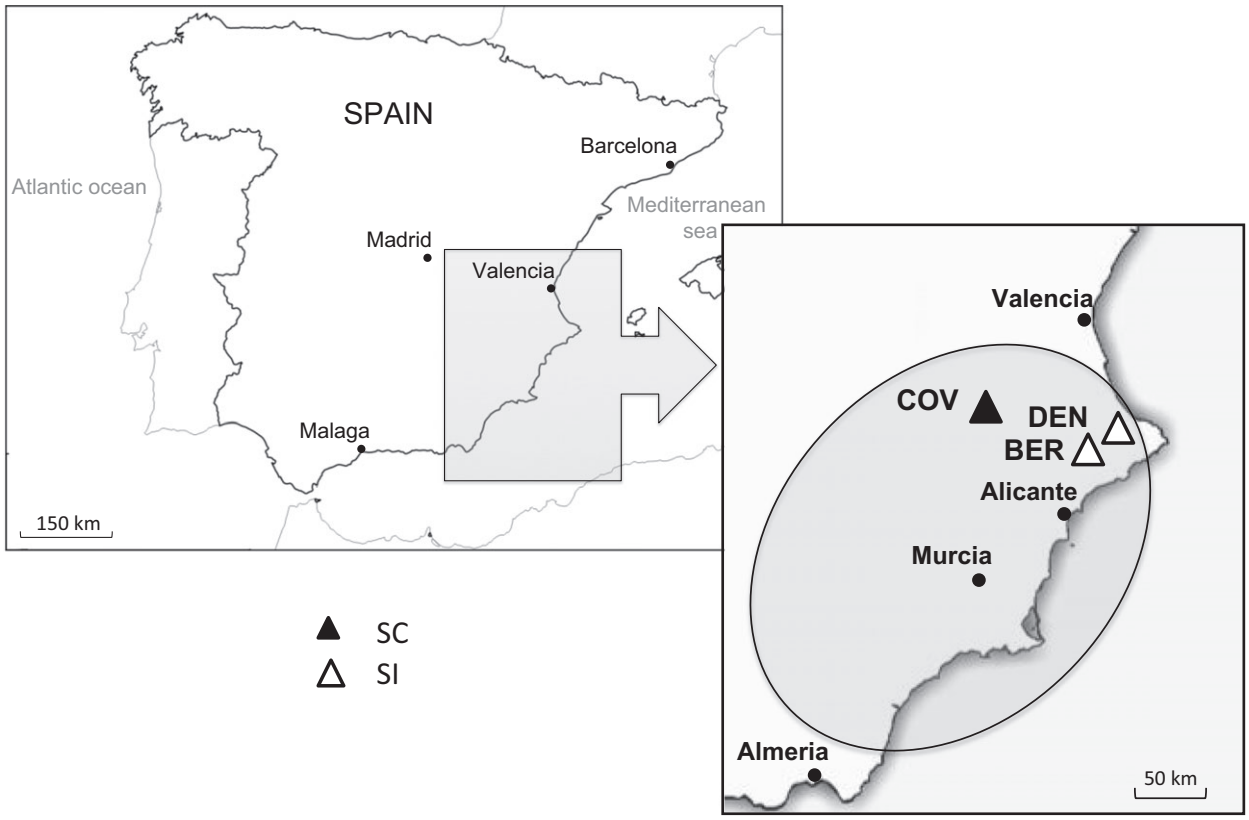

Fig. 1 Geographical range of *Linaria cavanillesii* in Spain (grey oval), and the populations that have been studied in detail (Voillemot & Pannell, 2016). Three northern populations (COV, DEN and BER) were used in the ABC simulations presented here. Their self-incompatibility status (SC: self-compatible; SI: self-incompatible) revealed by controlled crosses is indicated.

one cycle of 1 min at the annealing temperature and a final extension of 30 min at 72 °C. PCR products were then sequenced on an ABI3100 sequencer (Applied Biosystems, Foster City, CA, USA). We used the program Genemapper® to analyse microsatellite data.

ABC test of gene flow between natural populations

Two model comparisons were performed with ABC: (i) to test for the possibility of ongoing gene flow among the three sampled populations; and (ii) to test alternative topologies of population trees for the three populations. For each test, a specific ABC approach was adopted.

We tested the hypothesis of ongoing gene flow between *L. cavanillesii* populations by estimating the relative posterior probabilities of two models: the 'I model' (isolation) and the 'IM model' (isolation/migration). In the I model, an ancestral panmictic population becomes subdivided into two isolated daughter populations with no gene flow between them (Fig. 2). In the IM model, the two daughter populations remain connected by gene flow after an ancestral split (Fig. 2). Specifically, under the IM model, gene flow occurs in both directions at independent rates $M_i = 4N_i m$, where M_i is the number of migrants received each generation by population *i*, N_i is the effective population size of population *i*, and *m* is the proportion of individuals in population that were migrants from the other population the previous generation. The effective population sizes of the two current populations and the ancestral one were randomly sampled from a uniform prior distribution of [0–30 000] individuals and were allowed to vary freely to accommodate the occurrence of a bottleneck at the time of population divergence (T_{split}). T_{split} was sampled from a uniform prior of [0–100 000] generations. The scaled migration rate $4Nm$ under the IM model rate was sampled from the uniform prior of [0–20].

For each demographic model, we used the software ms to perform 10^6 multilocus coalescent simulations (Hudson, 2002). The program's output was then converted into microsatellite data sets on the basis of a generalized stepwise mutation model (GSM) assuming a mean mutation rate $\mu = 1.25 \times 10^{-5}$ (based on current estimates of the microsatellite mutation rate for plants; e.g. Vigouroux *et al.*, 2002; Marriage *et al.*, 2009). The probability of an increase or decrease in the microsatellite repeat number for each mutation was modelled assuming a geometrical parameter α distributed following a uniform prior and sampled on the interval [0–0.5]. For each simulated and observed data set, an array of summary statistics for polymorphism and divergence data was computed using publicly available R-scripts (Illera *et al.*, 2014; Rougemont *et al.*, 2016; https://github.com/QuentinRougemont/MicrosatDemogInference). The computed summary statistics correspond to the mean and standard deviation of the number of alleles over the 16 loci (*A*), the allelic richness (*Ar*), the observed and expected heterozygosities (H_o and H_e), the allele size in base pairs, the Garza-Williamson index (GW; Garza & Williamson, 2001), G_{ST} (Nei, 1973) and $\delta\mu_2$ (Goldstein *et al.*, 1995).

Relative posterior probabilities of the two models were estimated from comparisons between the vector of observed summary statistics and a reference table comprising summary statistics computed from 2 million simulations (one million simulations under each model). The 500 replicate simulations (out of 2×10^6) falling nearest to the observed summary statistic values were retained, and these were weighted by an Epanechnikov kernel that peaks when the observed

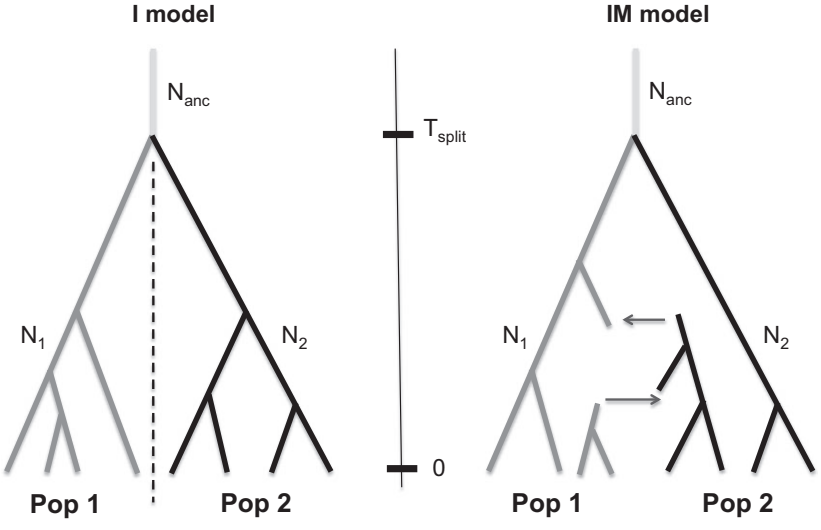

Fig. 2 Illustration of the two scenarios compared by ABC for the history of divergence among *Linaria cavanillesii* populations: the I model (isolation model) and the IM model (isolation and migration model). N_1, N_2 and N_{anc} are the number of effective individuals for each population. T_{split} is expressed in generations and represents the time since the ancestral subdivision.

statistic equals the simulated one. From the retained simulations, posterior probabilities of each model were estimated using a feed-forward neural network implementing a nonlinear multivariate regression by considering the model itself as an additional parameter to be inferred under the ABC framework, using the R package abc (Csilléry *et al.*, 2012). Computations were performed using 50 trained neural networks and 15 hidden networks in the regression. The robustness of the ABC model comparison (i.e. the probability of correctly supporting an M model given an estimated posterior probability P) was evaluated as follows. First, 1000 pseudo-observed data sets (PODs) were randomly simulated under each compared model using similar prior distributions. To estimate the relative posterior probabilities of each model, each simulated POD was then treated by ABC in a way similar to that of the *Linaria* data set. Finally, we estimated the robustness, R, of our inference on the basis of the obtained empirical distribution of the posterior probability P under the two models, with $R = P(P_I = P \mid I) / [\, P(P_I = P \mid I) + P(P_I = P \mid IM)]$. $P(P_I = P \mid I)$ is the probability of correct support for model I with the observed posterior probability P_I, and $P(P_I = P \mid IM)$ is the probability of wrongly supporting the I model with the observed posterior probability P, assuming here that the IM model is correct (Fagundes *et al.*, 2007).

DIYABC test of alternative topologies in population trees

The previously described approach is robust to test the existence of migration between two sampled gene pools, a feature not hitherto implemented in the software DIYABC (Cornuet *et al.*, 2014). However, preliminary analysis has shown that DIYABC has greater power to estimate parameters of a model with no gene flow (data not shown), and is able to deal with more than two populations. Thus, after rejecting the IM model (i.e. the hypothesis of ongoing gene flow; see Results), we tested alternative topologies describing possible evolutionary links between populations BER, COV and DEN using DIYABC (v.2.0.4) (Cornuet *et al.*, 2014) (Fig. 3a). Specifically, we compared three alternative topologies of a model involving divergence among three populations (Fig. 3a). This model describes the subdivision T_2 generations ago of an ancestral population of size N_5 into two populations, Pop 3 and Pop 4. Pop 3 has a constant effective population size N_3 from the time of the ancestral split up to the present. In contrast, Pop 4 of size N_4 is further split into the two daughter populations Pop 1 (of size N_1) and Pop 2 (of size N_2) T_1 generations ago (Fig. 3a). All sizes for current and ancestral populations were sampled independently, fully accommodating the possibility of either a bottleneck or an expansion at the time of divergence (T_1 and T_2). All three possible topologies of this model were compared, with Pop 3 identified as one of BER, COV or DEN (Fig. 3a). All topologies shared the same prior distributions and were randomly simulated 300 000 times, with parameter values sampled from uniform distributions. N_1, N_2, N_3, N_4 and N_5 were independently sampled from the uniform prior of [0–30 000]. The oldest time of divergence, T_2, was sampled from the uniform prior of [0–50 000] generations. Finally, T_1, the most recent time of divergence, was sampled for each iteration i from the uniform prior $[0–T_{2\text{-}i}]$, where $T_{2\text{-}i}$ is the sampled value for T_2 at the iteration i. We assumed a mutation rate of $\mu = 1.25 \times 10^{-5}$ for the GSM (Estoup *et al.*, 2002). Finally, we computed an array of summary statistics for each iteration obtained for all topologies. These statistics were as follows: the mean number of alleles; the genetic diversity (Nei, 1973); the mean allele size variance; the Garza-Williamson index (GW; Garza & Williamson, 2001); F_{ST} (Weir & Clark Cockerham, 1984); the mean classification index (Pascual *et al.*, 2007); the shared allele distance between populations (Chakraborty & Jin, 1993); and the $\delta\mu^2$ distance (Goldstein *et al.*, 1995).

The relative posterior probabilities of the three topologies were estimated using the logistic regression estimate implemented in DIYABC (Fagundes *et al.*, 2007; Beaumont, 2008) from the 1000 simulated data sets closest to the observed one. We then performed a goodness-of-fit test to evaluate the capacity of the estimated parameters to reproduce the observed data set under the best-supported scenario. We simulated 1000 data sets using a random combination of parameters sampled from the estimated joint posterior distribution, and we computed summary statistics for each simulated data set to obtain the expected distribution of the chosen statistics under the estimated scenario.

Results

Our ABC analysis strongly rejected a scenario of ongoing gene flow between the SC population COV and the two geographically nearby SI populations DEN ($P_{Isolation} = 1$; robustness = 1; Table 1) and BER ($P_{Isolation} = 1$; robustness = 1; Table 1). Our analysis also provides strong support for a scenario of ongoing gene flow between the two SI populations BER and DEN ($P_{Migration} = 0.80$; robustness = 1; Table 1). Note that the measures of robustness here represent the probability of correctly supporting the M model with the posterior probability estimated by ABC and can be interpreted as 1 minus the P-value.

Using the software DIYABC (Cornuet *et al.*, 2014), we compared different topologies of a three-population model of divergence (Fig. 3a). Two successive population splits were considered under this model, at two different times in the past T_1 and T_2, leading to three current populations from a single ancestral one. The best-supported topology corresponds to an ancestral

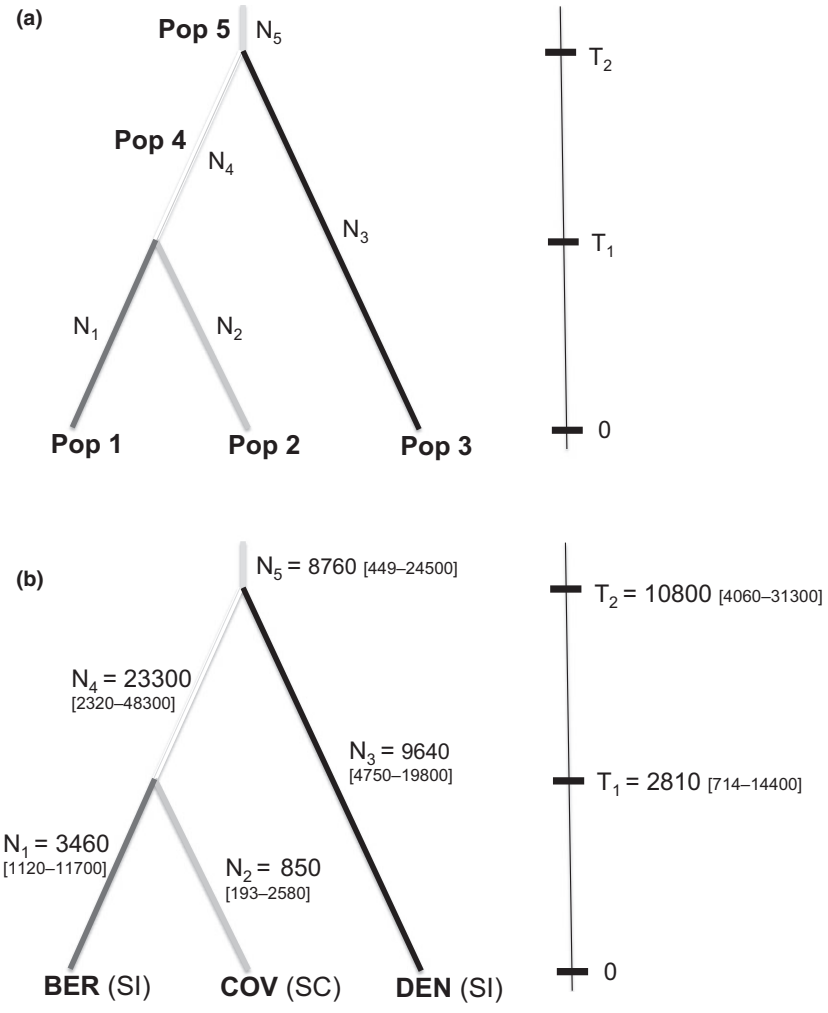

Fig. 3 (a) Illustration of competing scenarios of divergence for three populations of *Linaria cavanillesii*. We tested scenario 1: Pop 1 = DEN, Pop 2 = BER, Pop 3 = COV; scenario 2: Pop 1 = DEN, Pop 2 = COV, Pop 3 = BER; and scenario 3: Pop 1 = BER, Pop 2 = COV, Pop 3 = DEN. (b) Parameter estimation based on the best-supported scenario (scenario 3). N_1, N_2, N_3, N_4 and N_5 are the number of effective individuals in the respective populations; T_1 and T_2 are expressed in generations and represent the time of the ancestral subdivision. For each parameter estimate, 95% CI intervals are indicated in square brackets. The population incompatibility status is indicated: BER and DEN are self-incompatible (SI); COV is self-compatible (SC). See text for details.

Table 1 Model comparison between the I model (isolation model) and the IM model (ongoing migration model) using ABC simulations for three pairs of *Linaria cavanillesii* populations (COV, BER, DEN).

Population 1	Population 2	*P* (I model)	*P* (IM model)	Robustness
COV (SC)	DEN (SI)	1	0	1.0
COV (SC)	BER (SI)	1	0	1.0
BER (SI)	DEN (SI)	0.20	0.80	1.0

The posterior probabilities of the I model against the IM model obtained by ABC analysis are provided. The robustness is the probability that the best-supported model is indeed the correct one given the empirically observed posterior probabilities. Robustness was obtained using 1000 pseudo-observed data set and computing the posterior probabilities of each model by ABC analysis. Populations 1 and 2 refer to the population pair for which the corresponding models were compared. Incompatibility status is indicated in parenthesis for each population (SC: self-compatible vs. SI: self-incompatible).

split into two SI populations followed by a more recent split between the current SC population COV and the current SI population BER. This scenario is supported with a relative posterior probability of 0.61 [0.57–0.64]. The alternative scenarios 1 and 2 (Fig. 3a) are supported with relative posterior probabilities of 0.30 [0.27–0.33] and 0.09 [0.07–0.11], respectively.

Finally, we estimated the parameters describing the best-fitting topology using the same statistical framework implemented in DIYABC (Fig. 3b). With the assumed mutation rate of 1.25×10^{-5}, current effective population sizes were estimated as $N_{BER} = 3460$ (95% CI: 1120–11 700), $N_{COV} = 850$ (95% CI: 193–2580) and $N_{DEN} = 9640$ (95% CI: 4750–19 800) individuals (Fig. 3b). The ancestral split leading to the two current SI lineages occurred an estimated 10 000 generations ago (95% CI: 4060–31 300), whereas that leading to the current SC COV population occurred 2810 generations ago (95% CI: 714–14 400; Figs 3b and S2). Finally, we used a goodness-of-fit test to assess the

ability of a scenario with the estimated parameter values to reproduce the observed data set. The best-supported combination of scenario and associated parameter values was able to reproduce all of the 36 observed values of summary statistics (Table S1, Figs S3 and S4), suggesting that the proposed scenario is not only the best among the arbitrary set of compared scenarios, but is also able to explain faithfully most of the patterns of polymorphism and divergence observed among sampled natural populations of *L. cavanillesii*.

Discussion

We used ABC simulations to compare the fit of alternative demographic models of divergence to empirical data of the plant *L. cavanillesii*, a species with among-population variation in its SI status (Voillemot & Pannell, 2016). Overall, our analyses are consistent with a scenario where the lineage ancestral to COV (a mixed-mating population that has lost its SI system) has been diverging from ancestral SI populations for an estimated 2810 generations. Our analyses reject a scenario of ongoing gene flow between the SC and each of the two SI populations, but are consistent with a scenario of ongoing gene flow between the two SI populations. Our simulations also suggest that the effective population size of SC population is about ten times smaller than the SI populations and the inferred ancestral population. The inferred divergence time between DEN (SI) and the pair of populations COV (SC) and BER (SI) was nearly four times greater than between COV (SC) and BER (SI).

Accuracy and robustness of our results

Our inferences are necessarily based on very simple models of divergence. The utility of such ABC inference depends critically on the number of scenarios tested, as well as on whether the competing models can be accurately distinguished from one another. We believe that, despite their simplicity, the models explored are sufficiently different from one to another to provide a first-order insight into the history of divergence between *L. cavanillesii* populations. Moreover, our estimates of robustness based on ABC simulation indicate that the set of summary statistics chosen to describe the genetic data contains sufficient information to discriminate alternative scenarios. An uninformative set of statistics would lead to ambiguous model comparisons, with low variation of relative posterior probabilities among competing scenarios. Importantly, the best-supported scenario was able to reproduce all of the 36 statistics available to describe patterns of polymorphism and divergence in natural populations of *L. cavanillesii*. This gives us some confidence that much of the historical signal is captured in the selected scenarios. In particular, the absence of migration between the SC and SI populations points to strong genetic isolation and allows an estimate of the divergence time between the two populations.

In principle, we might have tested more complex models including periods of strict isolation followed by secondary contact. However, from our current simple sampling scheme with two or three populations and a limited number of microsatellite markers, increasing the number of model comparisons would have implied comparing submodels nested within those already chosen. For instance, our test for ongoing gene flow does not allow us to infer the origin of the putative migration: either the ongoing gene flow results from a secondary contact or results from continuous allelic exchanges since the populations split. Both theory (Alcala & Vuilleumier, 2014) and simulation studies (Roux *et al.*, 2016) show that these two submodels of ongoing gene flow can only be distinguished in extreme situations. For instance, strong statistical support for secondary contact is only possible for cases where it occurred relatively recently after a long period of isolation. One potentially important issue that we did not consider was the effect of a change in the mating system on population sizes and divergence times. Although selfing can compress coalescent times, the SC population is only partially selfing, and modelling has shown that coalescent trees for an SI population ($s = 0$) vs. one with intermediate selfing ($s = 0.5$) are difficult to distinguish (Nordborg & Donnelly, 1997), partly because a few generations of outcrossing are sufficient to erase signatures of inbreeding even in populations with a long history of selfing.

Our analysis suggests that the SC and the SI populations began to diverge relatively recently. This inference is of course sensitive to assumptions made for the mutation rate at markers chosen for the analysis. We assumed a microsatellite mutation rate of 1.25×10^{-5}, which corresponds to a lower bound of values estimated for other plant species (e.g. Vigouroux *et al.*, 2002; Marriage *et al.*, 2009). Lower mutation rates would of course elevate the estimated divergence time proportionally, but it is also possible that the mutation rate for *L. cavanillesii* was higher than that assumed, so that divergence times might also have been lower than inferred. Clearly, divergence time estimates based on other markers would be valuable, but it seems unlikely that the inferred recent divergence between SC and SI populations would be radically altered.

Our analysis arrived at evidently robust estimates for other model parameters, including the effective population sizes of the populations concerned and rates of migration between them. It is important to emphasize that these estimates are based on the assumption of uniformity in the population sizes and rates modelled. Migration and mutation rates are known to vary substantially across the genome (Hodgkinson & Eyre-Walker, 2011), and such variation has only recently

been included in demographic inference approaches (Cruickshank & Hahn, 2014; Roux *et al.*, 2016). Moreover, mutation rates, effective population sizes and migration rates in natural populations are also likely to be heterogeneous over time, and it is not clear how such variation might impact on the details of our results. Our estimates of the effective population sizes for the sampled populations seem implausibly high to us, given that the current census sizes are probably in the order of hundreds rather than thousands of individuals. However, the plants grow on cliffs, and it is possible that we missed subpopulations at inaccessible sites in the vicinity that may be connected by gene flow to the populations we sampled. Alternatively, exaggerated population size estimates might suggest that the mutation rate we assumed was too low. In this case, our estimates of divergence times would be even shorter than those in our analysis. Notwithstanding these uncertainties, the parameter values inferred here conform to patterns we might expect in relative terms, both in the light of theory (Nordborg & Donnelly, 1997; Charlesworth & Pannell, 2001) and conclusions reached from other studies (Glémin *et al.*, 2006; Wright *et al.*, 2008; Duminil *et al.*, 2009). In particular, the lower effective size of the SC population compared with the SI population is consistent with its lower genetic variation (Voillemot & Pannell, 2016), as well as with the expectation that selfing populations should have a lower N_e than outcrossing population in general (Nordborg & Donnelly, 1997; Charlesworth & Pannell, 2001; Roze & Rousset, 2004). The inferred genetic isolation (absence of ongoing gene flow) between the SC and the SI populations is also to be expected, because inbreeding populations tend to invest less in dispersal (reviewed in Charlesworth & Pannell, 2001; Barrett *et al.*, 2014) and thus to be more isolated from one another than outcrossing populations (Hamrick & Godt, 1996; Duminil *et al.*, 2009; Barrett *et al.*, 2014; but see below).

Implications for understanding the loss of SI in *L. cavanillesii*

Variation in the compatibility status among populations of *L. cavanillesii* is almost certainly due to the loss of SI rather than its gain (Schoen *et al.*, 1997; Igic *et al.*, 2006; Goldberg & Igić, 2008, 2012). We may thus suppose that the loss of SI in the lineage contributing to the SC population (COV) occurred at the time of, or after, its divergence from the SI populations from which it is derived, that is at least as recently as the inferred 2810 generations ago. *L. cavanillesii* is a long-lived perennial plant, with individuals that likely live for at least a decade in age-structured populations. Although it is difficult to estimate the generation time of *L. cavanillesii* accurately, if we allow for a mutations rate per year of up to ten times lower than that assumed in our analysis, the age of SC in the species is very plausibly less than 30 000 years. Given the relatively small size of the populations sampled and their inferred genetic isolation, especially the SC population, it is unlikely that they have persisted at the same localities over the entire period of their divergence. Our inference should thus be interpreted broadly; that is, the SC population corresponds simply to the lineage of plants that may have given rise to the sampled populations by colonization from elsewhere, possibly after the time of divergence inferred by our study. Such colonization would likely have reduced the effective size of the populations we sampled, a pattern consistent with the inferred effective population size of the SC population being about ten times smaller than the SI populations and the inferred ancestral population.

To what extent might the relatively recent loss of SI in *L. cavanillesii* account for the differences between the derived SC and the SI populations in terms of patterns of inbreeding depression (Voillemot & Pannell, 2017) and their floral biology (Voillemot & Pannell, 2016)? Although putative purging has been observed in many selfing SC species (e.g. Weber *et al.*, 2012; Dart & Eckert, 2013) and simulated under different conditions (e.g. Whitlock, 2002; Winn *et al.*, 2011; Marchini *et al.*, 2016), the dynamics of its evolution in natural populations is poorly known and difficult to assess. In *L. cavanillesii*, it seems likely that sufficient time has elapsed since the origin of SC for the population's genetic load to have been purged (Husband & Schemske, 1996; Crnokrak & Barrett, 2002). Indeed, Winn *et al.* (2011) performed simulations to see how quickly purging could occur after a transition to self-fertilization and found that even with low selfing rates, purging can occur rapidly (within a few hundred to thousand generations). However, it is not possible with our data to identify which factors were the main drivers of purging in our recently derived SC population: colonization through bottleneck, high selfing rates during colonization or a combination of both these scenarios could also contribute to the selection of SC and/or the purging of inbreeding depression. The relatively small population size, low genetic diversity and high population isolation of the SC population (Voillemot & Pannell, 2016) are all conditions that might accelerate the purging of deleterious alleles from a population (Kirkpatrick & Jarne, 2000; Whitlock, 2002; Pujol *et al.*, 2009; Oakley & Winn, 2012; Pekkala *et al.*, 2012; Lohr & Haag, 2015; Hedrick & Garcia-Dorado, 2016).

As noted in the Introduction, the autonomous SC population of *L. cavanillesii* shows no evidence for the evolution of a selfing syndrome (Voillemot & Pannell, 2016), that is a reduction in pollen production or allocation to attracting and rewarding pollinators (Ornduff, 1969; Sicard & Lenhard, 2011). One explanation could be that genetic variation in the SC lineage of *L. cavanillesii* was low, for example as a result of

population bottlenecks, and that it was thus unresponsive to selection. Alternatively, it could simply be that 3000 generations have been insufficient for the evolution a selfing syndrome. In their study using the hermaphrodite freshwater snail *Physa acuta*, Noël *et al.* (2016) found that although early-acting inbreeding depression was purged rapidly, male allocation remained unchanged over the 20-generation course of their experiment. In contrast, Bodbyl Roels & Kelly (2011) have shown that morphological changes relevant to a selfing syndrome can evolve within a few generations if there is sufficient variation upon which selection can act, a finding consistent with what is known more generally about the capacity of populations under natural selection to undergo rapid morphological change (e.g. Seeley, 1986; Losos *et al.*, 1997; Reznick *et al.*, 1997; Lendvai & Levin, 2003).

Other investigations of the divergence time among populations with contrasting mating systems have also inferred relatively recent transitions that are not associated with a selfing syndrome (e.g. Foxe *et al.*, 2010; Busch *et al.*, 2011). For instance, in SC populations of the perennial *A. lyrata*, the loss of SI occurred an estimated 10 000 years ago, and flowers still show an outcrossing syndrome (Hoebe *et al.*, 2009; Foxe *et al.*, 2010). Similarly, in the annual *L. alabamica*, a population that evolved SC 48 000 years ago displays only slight changes in floral size and pollen production (Busch *et al.*, 2011). These cases, and that of *L. cavanillesii*, contrast with that of the annual *Capsella rubella*, where a selfing syndrome has evolved in fewer than an estimated 20 000 years (Foxe *et al.*, 2009; Slotte *et al.*, 2012). It remains unclear why some species evidently evolve a selfing syndrome relatively rapidly, whereas others, such as *L. cavanillesii*, do not.

On balance, it seems to us implausible that the SC lineage of *L. cavanillesii* has been unresponsive to selection for increased selfing and reduced allocation towards pollinator attraction and reward for thousands of generations, but observations of other species referred to above clearly present a similar conundrum. Given that inbreeding depression has evidently been purged from the SC lineage of *L. cavanillesii* (Voillemot & Pannell, 2017), it is difficult to understand why selection should maintain outcrossing and an outcrossing syndrome in this particular case. It of course remains possible that SC evolved even more recently than the split between the lineages sampled, for example that the transition was facilitated by a severe bottleneck that depleted genetic variation, rendering the population unresponsive to selection for increased selfing.

Acknowledgments

We would like to thank Xavier Vekemans for suggesting the idea of the study. We also thank two anonymous reviewers for comments, and funding from the University of Lausanne to JRP in support of a studentship to MV. CR was supported by funds to JRP from the Swiss National Science Foundation.

All authors declare no conflict of interest and have seen and agreed to the submitted version of the manuscript, and no others are entitled to authorship.

References

Alcala, N. & Vuilleumier, S. 2014. Turnover and accumulation of genetic diversity across large time-scale cycles of isolation and connection of populations. *Proc. R. Soc. B Biol. Sci.* **281**: 20141369.

Baker, H.G. 1955. Self-compatibility and establishment after "long-distance" dispersal. *Evolution* **9**: 347–349.

Barrett, S.C.H. 2002. The evolution of plant sexual diversity. *Nat. Rev. Genet.* **3**: 274–284.

Barrett, S.C.H. & Charlesworth, D. 1991. Effects of a change in the level of inbreeding on the genetic load. *Nature* **352**: 522–523.

Barrett, S.C.H., Arunkumar, R. & Wright, S.I. 2014. The demography and population genomics of evolutionary transitions to self-fertilization in plants. *Philos. Trans. R. Soc. B Biol. Sci.* **369**: 20130344.

Beaumont, M.A. 2008. Joint determination of topology, divergence time, and immigration in population trees. In: *Simulation, Genetics, and Human Prehistory* (S. Matsumura, P. Forster & C. Renfrew, eds), pp. 135–154. McDonald Institute Press, Cambridge, UK. University of Cambridge.

Beaumont, M.A., Zhang, W. & Balding, D.J. 2002. Approximate Bayesian computation in population genetics. *Genetics* **162**: 2025–2035.

Bodbyl Roels, S.A. & Kelly, J.K. 2011. Rapid evolution caused by pollinator loss in *Mimulus guttatus*. *Evolution* **65**: 2541–2552.

Busch, J.W. 2005a. Inbreeding depression in self-incompatible and self-compatible populations of *Leavenworthia alabamica*. *Heredity* **94**: 159–165.

Busch, J.W. 2005b. The evolution of self-compatibility in geographically peripheral populations of *Leavenworthia alabamica* (Brassicaceae). *Am. J. Bot.* **92**: 1503–1512.

Busch, J.W. & Delph, L.F. 2012. The relative importance of reproductive assurance and automatic selection as hypotheses for the evolution of self-fertilization. *Ann. Bot.* **109**: 553–562.

Busch, J.W. & Schoen, D.J. 2008. The evolution of self-incompatibility when mates are limiting. *Trends Plant Sci.* **13**: 128–136.

Busch, J.W., Joly, S. & Schoen, D.J. 2011. Demographic signatures accompanying the evolution of selfing in *Leavenworthia alabamica*. *Mol. Biol. Evol.* **28**: 1717–1729.

Castric, V. & Vekemans, X. 2004. Plant self-incompatibility in natural populations: a critical assessment of recent theoretical and empirical advances. *Mol. Ecol.* **13**: 2873–2889.

Chakraborty, R. & Jin, L. 1993. A unified approach to study hypervariable polymorphisms: statistical considerations of determining relatedness and population distances. In: *DNA Fingerprinting: state of the Science* (S.D.L Pena, R. Chakraborty, J. Epplen & A.J Jeffreys, eds), pp. 153–175. Birkhäuser, Basel.

Charlesworth, D. & Charlesworth, B. 1979. The evolution and breakdown of S-allele systems. *Heredity* **43**: 41–55.

Charlesworth, D. & Charlesworth, B. 1987. Inbreeding depression and its evolutionary consequences. *Annu. Rev. Ecol. Syst.* **18**: 237–268.

Charlesworth, D. & Pannell, J. 2001. Mating systems and population genetic structure in the light of coalescent theory. In: *Integrating Ecology and Evolution in a Spatial Context* (J. Silvertown & J. Antonovics, eds), pp. 73–96. Blackwell Science, Oxford, UK.

Cheptou, P.-O. & Massol, F. 2009. Pollination fluctuations drive evolutionary syndromes linking dispersal and mating system. *Am. Nat.* **174**: 46–55.

Cornuet, J.M., Pudlo, P., Veyssier, J., Dehne-Garcia, A., Gautier, M., Leblois, R. *et al.* 2014. DIYABC v2.0: a software to make approximate Bayesian computations inferences about population history using single nucleotide polymorphism, DNA sequences and microsatellite, DNA data. *Bioinformatics* **30**: 1187–1189.

Crnokrak, P. & Barrett, S. 2002. Perspective: purging the genetic load: a review of the experimental evidence. *Evolution* **56**: 2347–2358.

Cruickshank, T.E. & Hahn, M.W. 2014. Reanalysis suggests that genomic islands of speciation are due to reduced diversity, not reduced gene flow. *Mol. Ecol.* **23**: 3133–3157.

Csilléry, K., Blum, M.G.B., Gaggiotti, O.E. & François, O. 2010. Approximate Bayesian computation (ABC) in practice. *Trends Ecol. Evol.* **25**: 410–418.

Csilléry, K., François, O. & Blum, M.G.B. 2012. Abc: an R package for approximate Bayesian computation (ABC). *Methods Ecol. Evol.* **3**: 475–479.

Dart, S. & Eckert, C.G. 2013. Experimental and genetic analyses reveal that inbreeding depression declines with increased self-fertilization among populations of a coastal dune plant. *J. Evol. Biol.* **26**: 587–599.

Dart, S., Samis, K.E., Austen, E. & Eckert, C.G. 2012. Broad geographic covariation between floral traits and the mating system in *Camissoniopsis cheiranthifolia* (Onagraceae): multiple stable mixed mating systems across the species range? *Ann. Bot.* **109**: 599–611.

Darwin, C.R. 1876. *The Effects of Cross and Self Fertilisation in the Vegetable Kingdom*. Murray, London, UK.

Duminil, J., Hardy, O.J. & Petit, R.J. 2009. Plant traits correlated with generation time directly affect inbreeding depression and mating system and indirectly genetic structure. *BMC Evol. Biol.* **9**: 177.

Estoup, A., Jarne, P. & Cornuet, J.M. 2002. Homoplasy and mutation model at microsatellite loci and their consequences for population genetics analysis. *Mol. Ecol.* **11**: 1591–1604.

Fagundes, N.J.R., Ray, N., Beaumont, M., Neuenschwander, S., Salzano, F.M., Bonatto, S.L. *et al.* 2007. Statistical evaluation of alternative models of human evolution. *Proc. Natl Acad. Sci.* **104**: 17614–17619.

Fenster, C. & Martén-Rodríguez, S. 2007. Reproductive assurance and the evolution of pollination specialization. *Int. J. Plant Sci.* **168**: 215–228.

Fisher, R. 1941. Average excess and average effect of a gene substitution. *Ann. Eugen.* **11**: 53–63.

Foxe, J.P., Slotte, T., Stahl, E.A., Neuffer, B., Hurka, H. & Wright, S.I. 2009. Recent speciation associated with the evolution of selfing in *Capsella*. *Proc. Natl Acad. Sci. USA* **106**: 5241–5245.

Foxe, J.P., Stift, M., Tedder, A., Haudry, A., Wright, S.I. & Mable, B.K. 2010. Reconstructing origins of loss of self-incompatibility and selfing in North American *Arabidopsis lyrata*: a population genetic context. *Evolution* **64**: 3495–3510.

Franklin-Tong, V.E. 2008. *Self-incompatibility in Flowering Plants. Evolution, Diversity and Mechanisms*. Springer, Berlin, Germany.

Garza, J.C. & Williamson, E.G. 2001. Detection of reduction in population size using data from microsatellite loci. *Mol. Ecol.* **10**: 305–318.

Glémin, S., Bazin, E. & Charlesworth, D. 2006. Impact of mating systems on patterns of sequence polymorphism in flowering plants. *Proc. R. Soc. B Biol. Sci.* **273**: 3011–3019.

Goldberg, E.E. & Igić, B. 2008. On phylogenetic tests of irreversible evolution. *Evolution* **62**: 2727–2741.

Goldberg, E.E. & Igić, B. 2012. Tempo and mode in plant breeding system evolution. *Evolution* **66**: 3701–3709.

Goldberg, E.E., Kohn, J.R., Lande, R., Robertson, K.A., Smith, S.A. & Igić, B. 2010. Species selection maintains self-incompatibility. *Science* **330**: 493–495.

Goldstein, D.B., Ruiz Linares, A., Cavalli-Sforza, L.L. & Feldman, M.W. 1995. Genetic absolute dating based on microsatellites and the origin of modern humans. *Proc. Natl Acad. Sci.* **92**: 6723–6727.

Goodwillie, C., Sargent, R.D., Eckert, C.G., Elle, E., Geber, M.A., Johnston, M.O. *et al.* 2010. Correlated evolution of mating system and floral display traits in flowering plants and its implications for the distribution of mating system variation. *New Phytol.* **185**: 311–321.

Guo, Y.-L., Bechsgaard, J.S., Slotte, T., Neuffer, B., Lascoux, M., Weigel, D. *et al.* 2009. Recent speciation of *Capsella rubella* from *Capsella grandiflora*, associated with loss of self-incompatibility and an extreme bottleneck. *Proc. Natl Acad. Sci.* **106**: 5246–5251.

Hamrick, J. & Godt, M. 1996. Effects of life history traits on genetic diversity in plant species. *Philos. Trans. R. Soc. B Biol. Sci.* **351**: 1291–1298.

Harder, L.D. & Barrett, S.C.H. 1995. Mating cost of large floral displays in hermaphrodite plants. *Nature* **373**: 512–515.

Harder, L.D. & Wilson, W.G. 1998. A clarification of pollen discounting and its joint effects with inbreeding depression on mating system evolution. *Amer. Nat.* **152**: 684–695.

Hedrick, P.W. & Garcia-Dorado, A. 2016. Understanding inbreeding depression, purging, and genetic rescue. *Trends Ecol. Evol.* **31**: 940–952.

Herlihy, C.R. & Eckert, C.G. 2002. Genetic cost of reproductive assurance in a self-fertilizing plant. *Nature* **416**: 320–323.

Hodgkinson, A. & Eyre-Walker, A. 2011. Variation in the mutation rate across mammalian genomes. *Nat. Rev. Genet.* **12**: 756–766.

Hoebe, P.N., Stift, M., Tedder, A. & Mable, B.K. 2009. Multiple losses of self-incompatibility in North-American *Arabidopsis lyrata*?: Phylogeographic context and population genetic consequences. *Mol. Ecol.* **18**: 4924–4939.

Holsinger, K.E. 1988. Inbreeding depression doesn't matter: the genetic basis of mating-system evolution. *Evolution* **42**: 1235–1244.

Hudson, R.R. 2002. Generating samples under a Wright-Fisher neutral model of genetic variation. *Bioinformatics* **18**: 337–338.

Husband, B.C. & Schemske, D.W. 1996. Evolution of the magnitude and timing of inbreeding depression in plants. *Evolution* **50**: 54–70.

Igic, B. & Kohn, J.R. 2006. The distribution of plant mating systems: study bias against obligately outcrossing species. *Evolution* **60**: 1098–1103.

Igic, B., Bohs, L. & Kohn, J.R. 2006. Ancient polymorphism reveals unidirectional breeding system shifts. *Proc. Natl Acad. Sci. USA* **103**: 1359–1363.

Igic, B., Lande, R. & Kohn, J.R. 2008. Loss of self-incompatibility and its evolutionary consequences. *Int. J. Plant Sci.* **169**: 93–104.

Illera, J.C., Palmero, A.M., Laiolo, P., Rodríguez, F., Moreno, Á.C. & Navascués, M. 2014. Genetic, morphological, and acoustic evidence reveals lack of diversification in the colonization process in an island bird. *Evolution* **68**: 2259–2274.

Jain, S. 1976. The evolution of inbreeding in plants. *Annu. Rev. Ecol. Syst.* **7**: 469–495.

Kirkpatrick, M. & Jarne, P. 2000. The effects of a bottleneck on inbreeding depression and the genetic load. *Am. Nat.* **155**: 154–167.

Lande, R. & Schemske, D.W. 1985. The evolution of self-fertilization and inbreeding depression in plants. I. Genetic models. *Evolution* **39**: 24–40.

Lande, R., Schemske, D.W. & Schultz, S.T. 1994. High inbreeding depression, selective interference among loci, and the threshold selfing rate for purging recessive lethal mutations. *Evolution* **48**: 965–978.

Layman, N.C., Fernando, M.T.R., Herlihy, C.R. & Busch, J.W. 2017. Costs of selfing prevent the spread of a self-compatibility mutation that causes reproductive assurance. *Evolution* **71**: 884–897.

Lendvai, G. & Levin, D. 2003. Rapid response to artificial selection on flower size in *Phlox*. *Heredity* **90**: 336–342.

Lloyd, D. 1965. *Evolution of Self-compatibility and Racial Differentiation in Leavenworthia* (Cruciferae), Contrib. from Gray Herb. **195**, 3–134. Harvard University, Cambridge, MA.

Lohr, J.N. & Haag, C.R. 2015. Genetic load, inbreeding depression, and hybrid vigor covary with population size: an empirical evaluation of theoretical predictions. *Evolution* **69**: 3109–3122.

Losos, J.B., Warheit, K.I. & Schoener, T.W. 1997. Adaptive differentiation following experimental island colonization in *Anolis* lizards. *Nature* **387**: 70–73.

Marchini, G.L., Cole, N.S., Ramakrishnan, A.P., Rosenthal, D.M. & Cruzan, M.B. 2016. Rapid purging of genetic load in a metapopulation and consequences for range expansion in an invasive plant. *Biol. Invasions* **18**: 183–196.

Marriage, T.N., Hudman, S., Mort, M.E., Orive, M.E., Shaw, R.G. & Kelly, J.K. 2009. Direct estimation of the mutation rate at dinucleotide microsatellite loci in *Arabidopsis thaliana* (Brassicaceae). *Heredity* **103**: 310–317.

Massol, F. & Cheptou, P.-O. 2011. Evolutionary syndromes linking dispersal and mating system: the effect of autocorrelation in pollination conditions. *Evolution* **65**: 591–598.

Nagylaki, T. 1976. A model for the evolution of self-fertilization and vegetative reproduction. *J. Theor. Biol.* **58**: 55–58.

Nei, M. 1973. Analysis of gene diversity in subdivided populations. *Proc. Natl Acad. Sci. USA* **70**: 3321–3323.

Ness, R.W., Wright, S.I. & Barrett, S.C.H. 2010. Mating-system variation, demographic history and patterns of nucleotide diversity in the tristylous plant *Eichhornia paniculata*. *Genetics* **184**: 381–392.

Noël, E., Chemtob, Y., Janicke, T., Sarda, V., Pélissié, B., Jarne, P. *et al.* 2016. Reduced mate availability leads to evolution of self- fertilization and purging of inbreeding depression in a hermaphrodite. *Evolution* **70**: 625–640.

Nordborg, M. & Donnelly, P. 1997. The coalescent process with selfing. *Genetics* **146**: 1185–1195.

Oakley, C.G. & Winn, A.A. 2012. Effects of population size and isolation on heterosis, mean fitness, and inbreeding depression in a perennial plant. *New Phytol.* **196**: 261–270.

Ornduff, R. 1969. Reproductive biology in relation to systematics. *Taxon* **18**: 121–133.

Pannell, J.R. 2015. Evolution of the mating system in colonizing plants. *Mol. Ecol.* **24**: 2018–2037.

Pannell, J.R., Auld, J.R., Brandvain, Y., Burd, M., Busch, J.W., Cheptou, P.-O. *et al.* 2015. The scope of Baker's law. *New Phytol.* **3**: 656–667.

Pascual, M., Chapuis, M.P., Mestres, F., Balanyà, J., Huey, R.B., Gilchrist, G.W. *et al.* 2007. Introduction history of *Drosophila subobscura* in the New World: a microsatellite-based survey using ABC methods. *Mol. Ecol.* **16**: 3069–3083.

Pekkala, N., Knott, K.E., Kotiaho, J.S. & Puurtinen, M. 2012. Inbreeding rate modifies the dynamics of genetic load in small populations. *Ecol. Evol.* **2**: 1791–1804.

Porcher, E. & Lande, R. 2005. The evolution of self-fertilization and inbreeding depression under pollen discounting and pollen limitation. *J. Evol. Biol.* **18**: 497–508.

Pujol, B., Zhou, S.-R., Sanchez Vilas, J. & Pannell, J.R. 2009. Reduced inbreeding depression after species range expansion. *Proc. Natl Acad. Sci. USA* **106**: 15379–15383.

Reznick, D.N., Shaw, F.H., Rodd, F.H. & Shaw, R.G. 1997. Evaluation of the rate of evolution in natural populations of guppies (*Poecilia reticulata*). *Science* **275**: 1934–1937.

Rougemont, Q., Roux, C., Neuenschwander, S., Goudet, J., Launey, S. & Evanno, G. 2016. Reconstructing the demographic history of divergence between European river and brook lampreys using approximate Bayesian computations. *PeerJ* **4**: e1910.

Roux, C., Fraïsse, C., Romiguier, J., Anciaux, Y., Galtier, N. & Bierne, N. 2016. Shedding light on the grey zone of speciation along a continuum of genomic divergence. *PLoS Biol.* **14**: e2000234.

Roze, D. & Rousset, F. 2004. Joint effects of self-fertilization and population structure on mutation load, inbreeding depression and heterosis. *Genetics* **167**: 1001–1015.

Runions, C.J. & Geber, M.A. 2000. Evolution of the self-pollinating flower in *Clarkia xantiana* (Onagraceae). I. Size and development of floral organs. *Am. J. Bot.* **87**: 1439–1451.

Schoen, D.J., Johnston, M.O., L'Heureux, A.-M. & Marsolais, J.V. 1997. Evolutionary history of the mating system in *Amsinckia* (Boraginaceae). *Evolution* **51**: 1090–1099.

Seeley, R.H. 1986. Intense natural selection caused a rapid morphological transition in a living marine snail. *Proc. Natl Acad. Sci. USA* **83**: 6897–6901.

Shimizu, K.K. & Tsuchimatsu, T. 2015. Evolution of selfing: recurrent patterns in molecular adaptation. *Annu. Rev. Ecol. Evol. Syst.* **46**: 593–622.

Sicard, A. & Lenhard, M. 2011. The selfing syndrome: a model for studying the genetic and evolutionary basis of morphological adaptation in plants. *Ann. Bot.* **107**: 1433–1443.

Slotte, T., Hazzouri, K. & Stern, D. 2012. Genetic architecture and adaptive significance of the selfing syndrome in *Capsella*. *Evolution* **66**: 1360–1374.

Stebbins, G. 1974. *Flowering Plants: evolution Above the Species Level*. Belknap Press of Harvard University, Cambridge, MA.

Stone, J.L., Vanwyk, E.J. & Hale, J.R. 2014. Transmission advantage favors selfing allele in experimental populations of self-incompatible *Witheringia solanacea* (Solanaceae). *Evolution* **68**: 1845–1855.
Tang, C., Toomajian, C., Sherman-Broyles, S., Plagnol, V., Guo, Y.-L., Hu, T.T. *et al.* 2007. The evolution of selfing in *Arabidopsis thaliana*. *Science* **317**: 1070–1072.
Vigouroux, Y., Jaqueth, J.S., Matsuoka, Y., Smith, O.S., Beavis, W.D., Smith, J.S.C. *et al.* 2002. Rate and pattern of mutation at microsatellite loci in maize. *Mol. Biol. Evol.* **19**: 1251–1260.
Voillemot, M. & Pannell, J.R. 2016. Maintenance of mixed mating after the loss of self-incompatibility in a long-lived perennial herb. *Ann. Bot.* **119**: 177–190.
Voillemot, M. & Pannell, J.R. 2017. Inbreeding depression is high in a self-incompatible perennial herb population but absent in a self-compatible population showing mixed mating. *Ecol. Evol.* **7**: 8535–8544.
Weber, J.J., Weller, S.G., Sakai, A.K., Nguyen, A., Tai, N.D., Domínguez, C.A. *et al.* 2012. Purging of inbreeding depression within a population of *Oxalis alpina* (Oxalidaceae). *Am. J. Bot.* **99**: 923–932.
Weir, B. & Clark Cockerham, C. 1984. Estimating *F*-statistics for the analysis of population structure. *Evolution* **38**: 1358–1370.
Whitlock, M.C. 2002. Selection, load and inbreeding depression in a large metapopulation. *Genetics* **160**: 1191–1202.
Winn, A.A., Elle, E., Kalisz, S., Cheptou, P.-O., Eckert, C.G., Goodwillie, C. *et al.* 2011. Analysis of inbreeding depression in mixed-mating plants provides evidence for selective interference and stable mixed mating. *Evolution* **65**: 3339–3359.
Wright, S. 1939. The distribution of self-sterility alleles in populations. *Genetics* **24**: 538–552.
Wright, S.I. & Barrett, S.C.H. 2010. The long-term benefits of self-rejection. *Science* **330**: 459–460.
Wright, S.I., Ness, R.W., Foxe, J.P. & Barrett, S.C.H. 2008. Genomic consequences of outcrossing and selfing in plants. *Int. J. Plant Sci.* **169**: 105–118.
Young, A. & Pickup, M. 2010. Low S-allele numbers limit mate availability, reduce seed set and skew fitness in small populations of a self-incompatible plant. *J. Appl. Ecol.* **47**: 541–548.

Supporting information

Additional Supporting Information may be found online in the supporting information tab for this article:
Table S1 Summary statistics from the ABC simulations.
Figure S1 Posterior probability for the time of split between the SC population (COV) and the five other known populations (BER, DEN, BUI, RUB, ZAR; respectively in red, yellow, green, blue and purple line).
Figure S2 Posterior probability for the time of split between populations COV and BER (red line), or between DEN and the combined pair COV-BER (blue line).
Figure S3 Distributions of estimated posterior probabilities.
Figure S4 Principal component analysis of summary statistics using 1000 data sets simulated with the prior distributions for the chosen parameters, the observed data and data from the posterior predictive distribution.

Received 23 April 2017; revised 3 November 2017; accepted 7 November 2017